6th European Conference on Computational Mechanics (ECCM 6)
7th European Conference on Computational Fluid Dynamics (ECFD 7)
11-15 June 2018, Glasgow, UK

ON ALLOWABLE STEP HEIGHTS: LESSONS LEARNED FROM THE F100 AND ATTAS FLIGHT TESTS

Geza Schrauf

DLR
Lilienthalplatz 7, 38108 Braunschweig, Germany
geza.schrauf@dlr.de

Key words: Laminar Flow Technology, Laminar-Turbulent Boundary Layer Transition, Surface Quality, Forward and Backward Facing Steps, Roughness.

Abstract. Data and observations from F100 and ATTAS flight tests with forward and backward facing steps are presented and a modification of a classical step criterion is proposed.

1 INTRODUCTION

Laminar flow technology for wings, tail surfaces, and nacelles promises considerable drag reduction. Its application requires sufficiently smooth surfaces to avoid premature transition to turbulence. For industrial application we emphasize that "sufficiently smooth" is enough, because requiring a very high surface quality "just to be on the safe side" would make the manufacturing of laminar surfaces prohibitively expensive.

We distinguish between the following four types of surface quality issues:

- surface waviness,
- distributed roughness or sand paper roughness,
- three-dimensional roughness elements such as rivet heads or insect debris,
- two-dimensional roughnesses such as forward or backward facing steps and gaps.

A surface wave has a relatively large extension and modifies the pressure distribution. Therefore, its influence on transition can be estimated with boundary layer and linear stability computations.

Distributed roughness, in contrast, comes from the surface finishing. It consists of very small 3D disturbances which influence the near-wall region of the boundary layer. They are not visible in the pressure distribution. The engineering approach is to use criteria based on simple roughness numbers such as R_a, R_t, R_q, and R_z. This, however, is not adequate. The reasons will be discussed at another time.

Figure 1: Fokker F100 with laminar flow glove on starboard wing

3D roughness elements, such as rivet heads and insect debris, can be analyzed with the help of Direct Numerical Simulation (DNS) which provides a visualization, and with that, an understanding of the vortical flow behind the disturbance.

Finally, a 2D roughness such as a forward or backward facing step, can also by studied using DNS. Another possibility would consist of a Navier-Stokes calculation with sufficient resolution to resolve the local separation regions, with subsequent linear stability analysis to show the effect on transition.

However, those methods are too time-consuming and expensive for the design process. Instead a set of simple criteria can be used to allow fast design decisions.

In this paper we will apply the classical Nenni-Gluyas criteria [1] for backward and forward steps to the results of flight measurements. We prefer to modify* the criteria and to use them in the following form:

$$Re_h = \frac{U_e\, h}{\nu_e} = 900, \qquad \text{(C1mod)}$$

$$Re_h = \frac{U_e\, h}{\nu_e} = 1800. \qquad \text{(C2mod)}$$

Furthermore, we propose a modification of these simple criteria using linear stability theory.

2 F100 FLIGHT TESTS

Within the European ELFIN I project, a natural laminar flow (NLF) glove was mounted on the starboard wing of a Fokker F100 aircraft to demonstrate that natural laminar flow can be achieved on a smaller transport aircraft flying at Mach 0.75 [2]. After the completion of the flight tests in May 1992 [3], additional flight tests were performed within the follow-on LARA project to investigate the effect of 2D and 3D roughnesses on the laminar-turbulent transition. Two flights were performed simulating forward facing steps (FFSs) by applying foils on the upper surface of the wing:

*The original Nenni-Gluyas criteria (C1) and (C2) are based on the free-stream data, i.e. $U_\infty\, h\,/\,\nu_\infty$, instead of the data at the edge of the boundary layer.

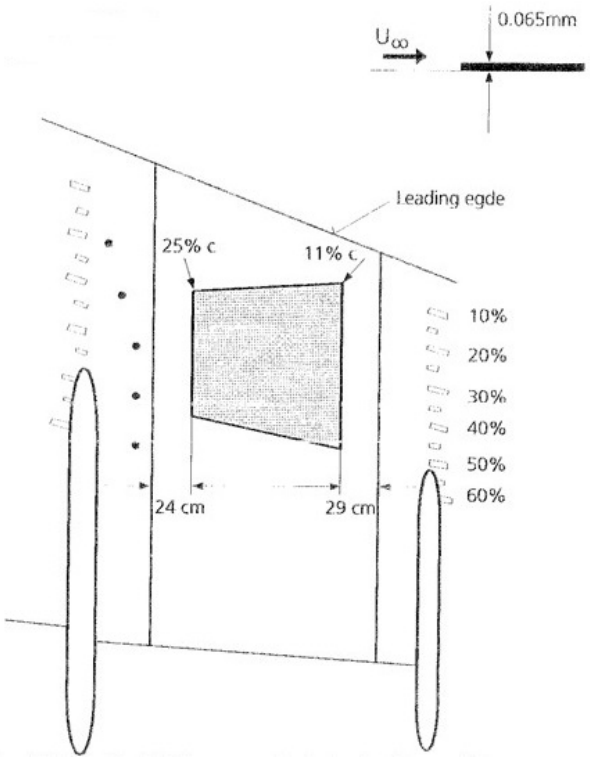

Figure 2: Arrangement of the foils on the upper side of the starboard wing

1 June 1992: Flight 5 with foil thickness 0.065 mm, measurement numbers 5xx.
4 June 1992: Flight 6 with foil thickness 0.170 mm, measurement numbers 6xx.

At that time, only a qualitative quick-look analysis of the infrared images was done [4]. Now we want to do a quantitative evaluation. The measured pressure distributions obtained from the LARA flight tests are not smooth enough in the immediate neighborhood of the stagnation point to allow the determination of the effective sweep angle [5]. Thus, we modified the LARA pressure distributions in the immediate neighborhood of the stagnation point so that a re-calculation of the effective sweep angle would result in the effective sweep angle of a corresponding ELFIN case.

We remind that a small change of the effective sweep angle will mostly affect the computed cross-flow N-factors and not the Tollmien-Schlichting N-factors. Therefore, these small modifications will not affect the results because the forward facing steps considered here have a dominant influence on Tollmien-Schlichting (TS) transition.

For the analysis we compute the functions

$$x \longrightarrow Re_{h=0.065mm} = \frac{U_e}{\nu}_e \, 0.065mm, \tag{1}$$

$$x \longrightarrow Re_{h=0.17mm} = \frac{U_e}{\nu}_e \, 0.17mm, \tag{2}$$

and evaluate them at $X/C = 0.11$ for the outboard pressure distribution and at $X/C = 0.25$ for the inboard one. From the infrared images we can see whether or not the step has

Table 1: Corresponding pairs of flight measurements without and with a $0.17mm$-step.

Flight	Step	Ma_∞	$Re^\dagger * 10^{-6}$	C_L	β	Transition Location	
						Inner Section	Outer Section
329	clean	0.748	20.6	0.391	3.544	33%	35%
613	FFS	0.748	20.9	0.395	3.610	Unclear Image	
341	clean	0.748	17.5	0.477	0.257	21%	20%
619	FFS	0.750	16.7	0.471	0.062	24%	29%
437	clean	0.753	17.2	0.465	2.272	30%	33%
621	FFS	0.750	16.5	0.473	2.248	31%	35%
443	clean	0.805	19.8	0.384	0.346	>55%	40%
623	FFS	0.799	19.7	0.382	-.031	>55%	42%

had an influence on transition. Additionally, we enhance the assessment of the transition with accompanying linear stability calculations.

To assess the effect of the forward facing step we look for pairs of flight measurements from ELFIN I and LARA with the same Mach and Reynolds numbers, the same lift coefficients and the same sideslip angles. For the larger forward facing step of $0.17mm$, we have four suitable pairs of test cases which are listed in Table 1.

3 FLIGHT MEASUREMENTS 329 & 613

We begin our evaluation with the infrared images of flight measurements 329 and 613 which are shown in Figure 3. Our first impression is that, on the outboard side, transition occurs for both cases between 40% and 45% chord. Furthermore, already at around 20% something seems to happen. On the inboard side, transition is observed before the step at 15%. Therefore, we conclude that the $0.17mm$-step does not affect transition.

To better understand the infrared images, we perform boundary layer and stability calculations with [6] and [7]. The N-factors obtained with incompressible, linear stability theory for the outer section of the two flight measurements are shown in Figure 4.

The pressure distribution of the outer section has a bump at 20% which is probably caused by a wave in the glove surface. From the infrared image of case 613 we see that this wave extends in spanwise direction over the whole glove surface and reaches the inboard section at 15% chord. This is in line with a bump observed in the measured pressures (cf. Figure 6). Due to the waviness of the surface, the envelope of the N_{TS}-factors exhibits two local peaks, one with $N_{TS} = 10.5$ at 20% chord and a second one with the somewhat higher N_{TS}-value of 11 at 42% chord. From the comparison with the infrared image we see that transition occurs at the second peak, probably due to non-linear effects. In Figure 4

†The Reynolds numbers are computed with the aerodynamic mean chord of $3.5m$, not with the local chord lengths.

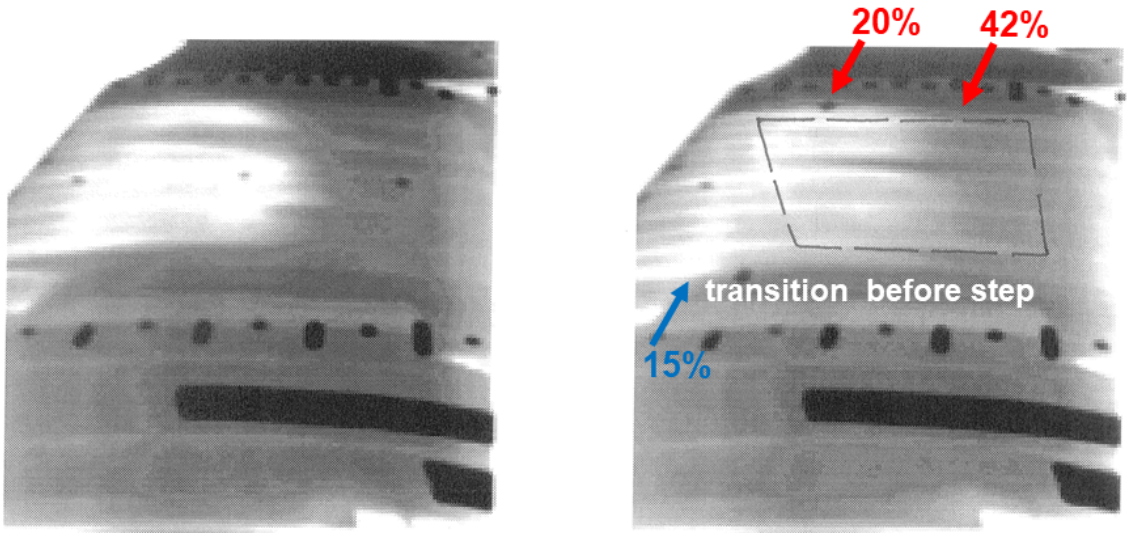

Figure 3: Infrared images of F329 & F613.

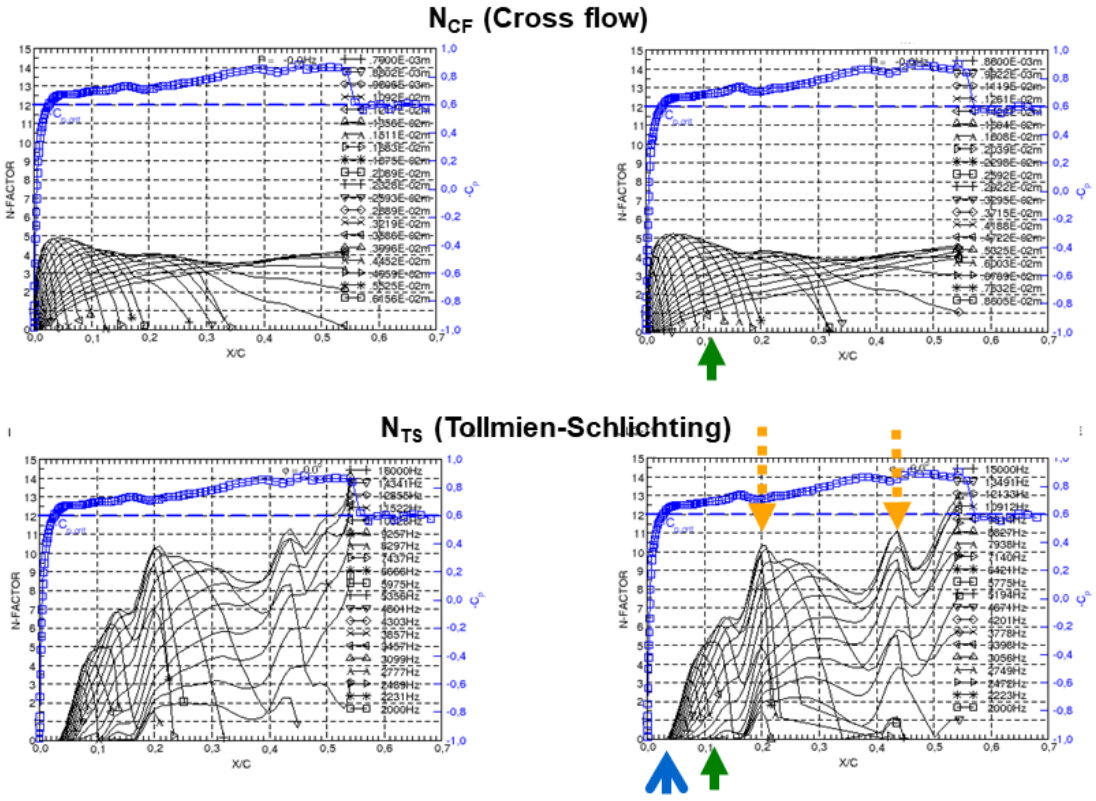

Figure 4: Stability analysis of the outboard section of 329 & 613.

we have marked the location of the step at 11% chord with a green arrow. We see that the step is located in a region of very rapidly growing TS-waves between the neutral point,

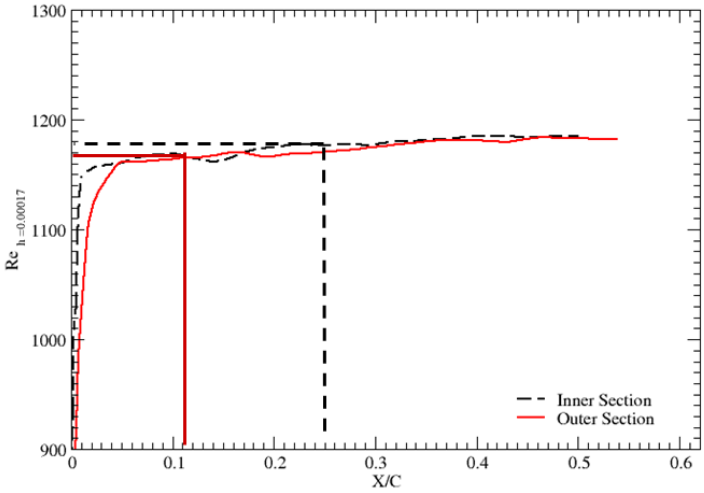

Figure 5: The functions (1) and (2) for measurement 613.

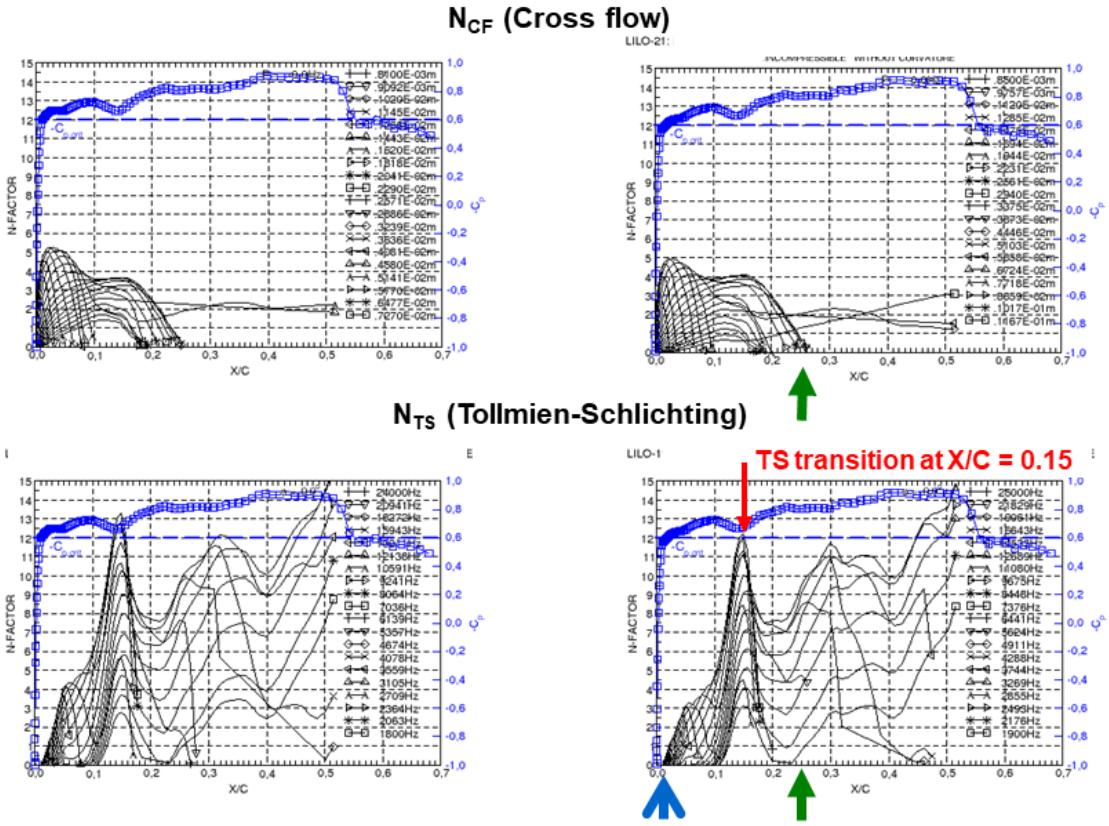

Figure 6: Stability analysis of the inboard section of 329 & 613.

marked with the blue arrow, and the first N_{TS}-factor peak.

The function $x \longrightarrow Re_{h=0.170mm}$ is shown in Figure 5. Its value at 11% is around

1170 so that this step should not cause transition according to the classical criterion of Nenni & Gluyas [1]. This is consistent with what we observed during the flight tests. In Figure 6, we present the N-factors computed for the measured pressure distribution of the inboard section. We observe a strong peak in the N_{TS}-factors at 15% which obviously causes transition already before the step. This can be seen from the infrared image. The peak is caused by the aforementioned wave in the surface which seems to be stronger on the inboard side.

From this discussion we see that it might be difficult to interpret the transition behavior from an infrared image alone. It would be much better to perform a stability analysis already during the flight test campaign, to be able to compare the N-factor results with the infrared images. Today this should be possible, in view of the much increased computing power and the code improvements, especially for automatized boundary layer and stability analysis.

4 RESULTS FOR THE LARGER STEP

In the four cases of the Table 1, the step of 0.170 mm had no effect on transition. The Reynolds numbers Re_h of these cases are listed in the Table 2. These results are in

Table 2: Reynolds numbers Re_h for the cases with the 0.170 mm-step

Flight	Re_h
613	1160 - 1180
619	940 - 950
621	930 - 940
625	1170

line with criterion (C2mod). Unfortunately, there was no opportunity to perform another flight with a larger step.

5 RESULTS FOR THE SMALLER STEP

The test flight with the smaller step of height 0.065 mm was performed first. A list with corresponding pairs of flight measurements without and with the step is given in Table 3. We expected that the smaller step should have less impact. This is reflected in the smaller Re_h numbers listed in Table 4.

However, the flight measurement 511 is somewhat ambigous. Its infrared image is shown in Figure 7 and one might detect a forward moving transition near the outboard edge of the foil. This case was intensely discussed and it remained unclear whether the step had an influence on transition. Taking into account the small Re_h number and considering that all the other cases had no effect on transition, the author claims that also in case 511, transition was not affected by the step. What is seen in the infrared image might be caused by different contrast settings of the infrared camera.

Table 3: Corresponding pairs of flight measurements without and with a 0.065mm-step.

Flight	Step	Ma_∞	$Re^\ddagger * 10^{-6}$	C_L	β	Transition Location	
						Inner Section	Outer Section
407	clean	0.721	27.0	0.297	0.105	32%	27%
507	FFS	0.716	26.0	0.296	0.062	32%	25%
409	clean	0.719	26.9	0.294	2.851	36%	30%
509	FFS	0.719	26.1	0.296	3.061	33%	26%
443	clean	0.805	19.8	0.384	0.346	>55%	40%
525	FFS	0.807	21.1	0.342	0.338	39%	40%
455	clean	0.719	26.9	0.294	2.851	36%	30%
531	FFS	0.719	26.1	0.296	3.061	33%	26%
413	clean	0.747	26.0	0.301	2.952	35 - 51%	31 - 50% i
511	FFS	0.746	25.5	0.313	2.645	43%	30%
431	clean	0.762	20.2	0.396	2.272	>55%	37%
517	FFS	0.768	20.6	0.390	2.226	>55%	35%

Table 4: Reynolds numbers Re_h for the cases with the 0.065 mm-step.

Flight	Re_h
507	550 - 560
509	550 - 560
525	430 - 440
531	520 - 540
511	530 - 540
517	430 - 440

The dispute on this measurement shows that a qualitative evaluation already during the flight test campaign would have been very beneficial.

6 ATTAS FLIGHT TESTS

The aim of the ATTAS flight tests was to produce boundary layer transition data for the N-factor correlation of linear stability theory. Therefore, the geometry of the glove did not represent a typical laminar wing but was designed for monotonically increasing envelopes of the N_{CF}- and N_{TS}-factors. The outcome of the N-factor correlation can be found in [3].

‡The Reynolds numbers are computed with the aerodynamic mean chord of 3.5m, not with the local chord lengths.

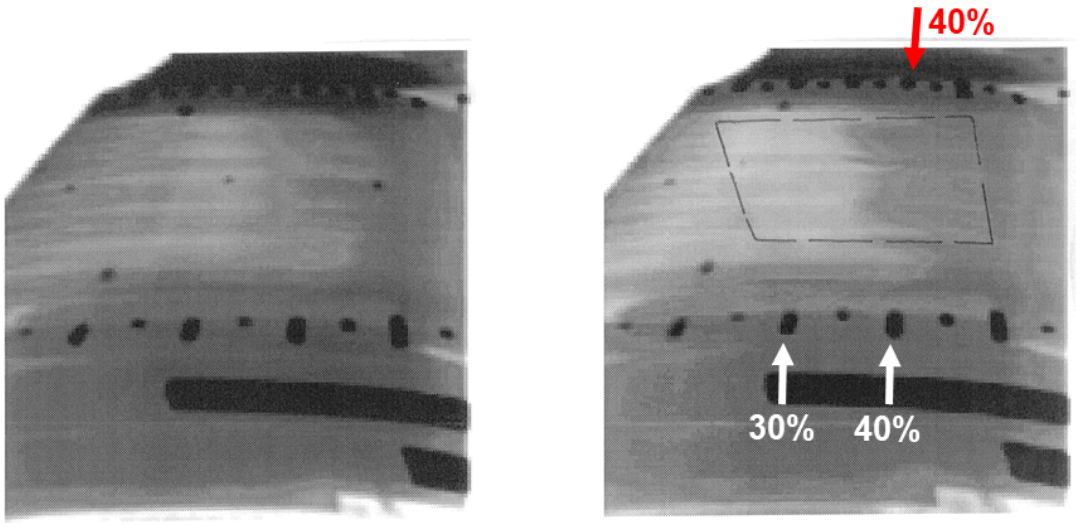

Figure 7: Infrared images of F413 & F511.

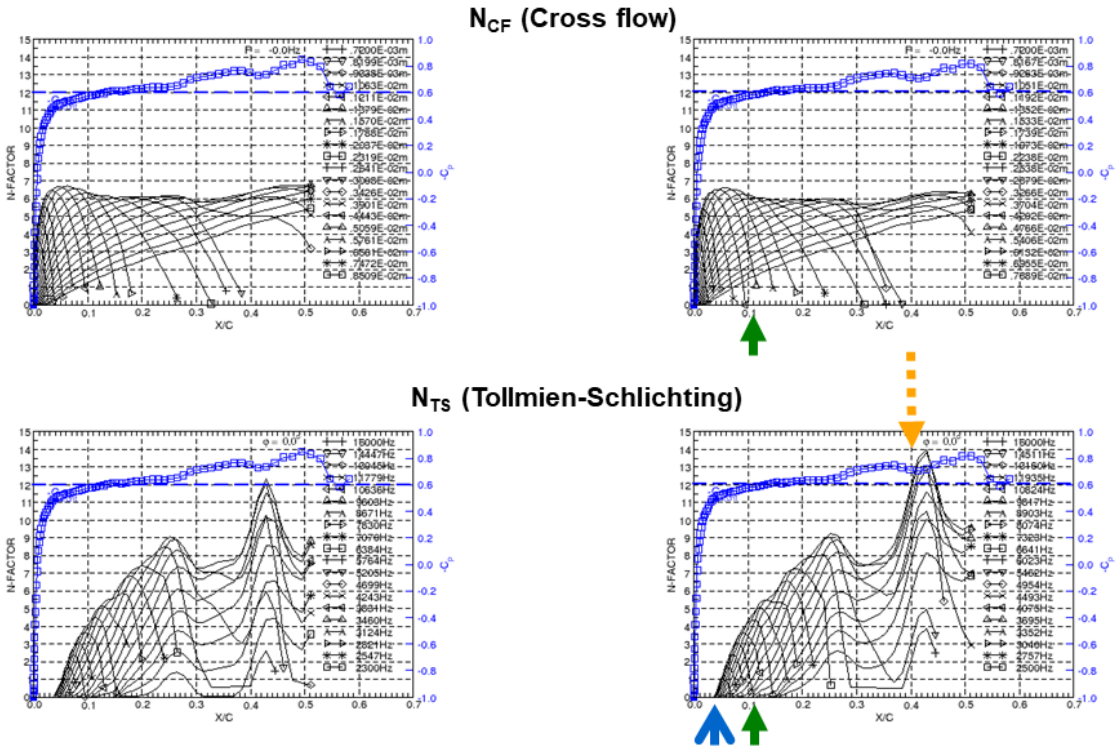

Figure 8: Stability analysis of the outboard section of 413 & 511.

Compared to a typical laminar wing, the neutral point for TS-amplification is situated more downstream, often at around 10% chord.

In addition to the flights for the N-factor correlation, two flights were performed with

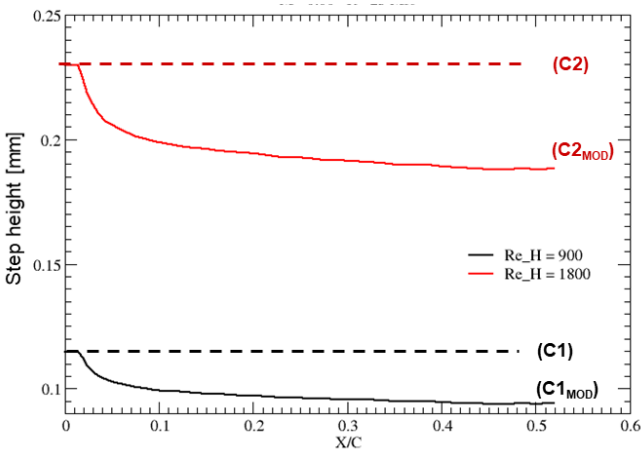

Figure 9: Step heights for a representative ATTAS flight test case

stripes of adhesive tape attached to the surface to simulate steps. The stripes had a thickness of 0.05 mm, a width of 19 mm and a length of 500 mm. One flight was performed with the stripes attached along constant X/C-lines at the locations $X/C = 0.05, 0.10$ and 0.15, the other one with the stripes at the locations $X/C = 0.20, 0.25$ and 0.30. The flow passed across each stripe with its two edges: the first edge provided a forward facing step (FFS), and the second, a backward facing step (BFS).

Because the pressure acquisition system failed during those flights, we can only report on the qualitative behavior. Using the pressure distribution from similar N-factor-correlation flights we estimate the allowable step heights for both forward and backward steps according to the original (C1, C2) and the modified (C1mod, C2mod) Nenni-Gluyas criteria[§] (cf. Figure 9). We see that an FFS with a height of $0.05mm$ is uncritical beyond doubt. Therefore, if there is an effect, we assume that stripe is acting as a BFS.

During the flights, we observed the following behavior on transition:

(A)	Tape at $X/C = 0.05$:	no effect on transition.
(B)	Tape at $X/C = 0.10,\ 0.15$:	transition moved forward.
(C)	Tape at $X/C = 0.20,\ 0.25, 0.30$:	small or no effect on transition.

Even though the boundary layer is thinnest at the location $X/C = 0.05$, no effect was observed. This is because the tape was located upstream of the neutral point so that the disturbances introduced by the BFS were damped. Placed upstream of the neutral point, a BFS has no effect or must be large enough to trigger a by-pass transition.

The strongest effect was observed in case (B). In this case the BFS was located in the neighborhood of the neutral point of the TS-waves. At this location, the disturbances introduced by the BFS have the maximal potential for further amplification.

In case (C), there was a less pronounced effect, or no effect, even though, according to the criterion (C1mod) the BFS should have been more critical. The author's explanation

[§]In Figure 9 we use the original criterion to limit the step height computed with the modified criterion because $h \longrightarrow \infty$ if $U_e \longrightarrow 0$.

for this behavior is that there is simply less amplification potential between the more downstream position of the step and the transition location of the clean wing.

This shows that a criterion for the effect of a step on transition should take the stability of the boundary layer at and behind the step into account. If the step does not trigger by-pass transition, then the strongest influence should occur in situations with moderate TS-growth over a long distance behind the step and before the transition location of the clean wing. In view of this, the author proposes to modify the criteria with the help of N_{TS}-factors which are anyhow available during laminar flow design.

Furthermore, these results indicate that the Reynolds number in the criterion (C1mod) should not be increased.

7 PROPOSAL A MODIFIED CRITERIA

The so-called ΔN-methods [8, 9, 10, 11] constitute one approach to include the stability behaviour. A step with a certain height h will introduce additional disturbances into the boundary layer. They increase the N_{TS}-factors by an ΔN which is assumed to be function of h and of other parameters, i.e. $\Delta N = f(h; p_1, p_2, \ldots)$. The "critical" N_{TS}-value for transition will then be reached earlier indicating a shift forward of the transition location. In our opinion it is very difficult to determine a suitable function $\Delta N = f(h; p_1, p_2, \ldots)$.

Therefore, we propose not look for such a function but to use the N-factor results to specify a range of validity for the criteria (C1mod) and (C2mod). With this in mind, we propose the following procedure.

First, we determine the allowable step height by

$$h_{BFS} \leq Re_{BFS}\ \nu_e/U_e \quad \text{for a BFS,} \tag{3}$$

$$h_{FFS} \leq Re_{FFS}\ \nu_e/U_e \quad \text{for a FFS.} \tag{4}$$

For a BFS, we take $Re_{BFS} = 900$. However, because the classical value of $Re_{FFS} = 1800$, for the FFS is often too conservative for laminar design, we propose to double the value, i.e to use $Re_{FFS} = 3600$[¶].

Next, we restrict the range of validity of the modified criteria as follows: find the first location $X_{N_{TS}=4}$ where the N_{TS}-envelope reaches the value 4 and apply the criteria only downstream of this locations, i.e. for $X > X_{N_{TS}=4}$.

Finally, we only claim that the allowable step heights obtained from the criteria are safe in the sense that they do not cause transition. The computed step heights are by no means "sharp".

The range restriction has two implications. First, we exclude the neighborhood of the neutral point, where the boundary layer is very sensitive to surface imperfections. Second, we increase the value of Re_{FFS} to allow larger forward facing steps.

Avoiding the neighborhood of the neutral point, where the surface should be as smooth as possible, is not a drawback. In many practical applications for natural laminar flow, the

[¶]Sometimes even this value is conservative.

leading edge is made out of one integral part and the first step occurs at the connection of this part to a front spar. The location $X_{N_{TS}=4}$ is generally ahead of the front spar.

For hybrid laminar flow we need some adaptation. Due to suction, TS-amplification normally starts behind the front spar, so that the range $X > X_{N_{TS}=4}$ does not include the area of interest.

REFERENCES

[1] Nenni, J.P., Gluyas, G.L., Aerodynamic design and analysis of an LFC surface. *Astronautics and Aeronautics* (July 1966) 52-57.

[2] Schrauf, G., Status and perspective of laminar flow. *The Aeronautical Journal* (2005) **1051.102**:639-644.

[3] Schrauf, G., Large-scale laminar flow tests evaluated with Linear stability theory. *AIAA Journal of Aircraft* (2004), **41.2**:224–230.

[4] Rohard, C.-H., Horstmann,K.H., Evaluation of infra-red pictures with respect to the influence of surface roughness on transition on Fokker F100 laminar wing glove. LARA Technical Report 26 (December 1994).

[5] Schrauf, G., A note on the calculation of the effective sweep angle and the attachment line Reynolds number. ELFIN II Technical Report 116 (January 1994).

[6] Schrauf, G., COCO - A program to compute velocity and temperature profiles for local and non-local stability analysis of compressible, conical boundary layers with suction. ZARM Technical Report, November 1998.

[7] Schrauf, G. LILO 2.1 - User's guide and tutorial. GSCS Technical Report 6, orig. issued September 2004, modified for version 2.1 June 2006.

[8] Crouch, J.D., Ng, L.L., Variable N-factor method for transition prediction in three-dimensional boundary layers. *AIAA Journal* (2000), **38.2**:211–216.

[9] Crouch, J.D., Kosorygin, V.S., Ng, L.L., Modelling the effects of steps in boundary-layer transition In: Govindarajan, R.i(ed), Sixth IUTAM Symposium on Laminar-Turbulent Transition (2006), Springer, 37–44.

[10] Perraud, J., Séraudie, A, Effects of steps and gaps and and 3D transition. ECCOMAS 2000, Barcelona, Spain.

[11] Perraud, J., Arnal, D., Séraudie, A, Tran, D, Laminar-turbulent transition on aerodynamic surfaces with imperfection. RTO-MP-AVT 111 (2004).